Aberrant ROS Served as an Acquired Vulnerability of Cisplatin-resistant Lung Cancer

Qian Xin
Shandong University Cheeloo College of Medicine
Qinghong Ji
Shandong University Cheeloo College of Medicine
Ying Zhang
cheeloo college of medicine
Weihong Ma
cheeloo college of medicine
Baoqing Tian
Shandong cancer hospital
Yanli Liu
Shandong Cancer Hospital
Yunsong Chen
Shandong Cancer Hospital
Fei Wang
Shandong Cancer Hospital
Ran Zhang
Shandong Cancer Hospital
Xingwu Wang
Shandong Cancer Hospital
Jupeng Yuan (yuanjupeng1988@gmail.com)
Shandong Provincial Key Laboratory of Radiation Oncology, Cancer Research Center, Shandong Cancer Hospital and Institute, Shandong First Medical University and Shandong Academy of Medical Sciences, Jinan, Shandong, 250117, P.R. China. https://orcid.org/0000-0003-1817-7771

Research

Keywords: APR-246, Lung cancer, Cisplatin resistance, Reactive oxygen species, NRF2, SLC7A11

Posted Date: January 8th, 2021

DOI: https://doi.org/10.21203/rs.3.rs-141062/v1

Abstract

Background

Lung cancer has become a global health issue in recent decades. Despite of high rate of resistance, cisplatin-base chemotherapy is still the main treatment of lung cancer patients who are not suitable for TKI-based targeted therapy and immunotherapy. Thus, overcoming cisplatin resistance is urgently needed.

Methods

A small panel is established to screen chemicals and compounds overcoming cisplatin resistance. Survival fractions as well as proliferation are determined by MTT assay. Colony formation assay, JC-1 assay, EdU assay, ROS assay as well as apoptosis and cell cycle assay are performed to verify vitalities of different groups. Quantifications of NADP+/NADPH and GSH/GSSG are carried out according to standard protocols. Xenograft model is generated to evaluate the *in vivo* role of APR-246.

Results

In this study, we identify NADPH metabolism and reactive oxygen species (ROS) levels as the main cause accounting for cisplatin resistance of H460. Based on a small panel consisting common chemotherapy drugs and compounds, APR-246 is proved an effective compound specifically inhibiting proliferation and colony formation of cisplatin resistant H460 (H460-Cis) cells. APR-246 significantly causes G0/G1 accumulation and S phase inhibition of H460-Cis cells. Besides, APR-246 can obviously lead to severe mitochondria dysfunction as well as elevated apoptosis by altering apoptosis-related protein expressions in H460-Cis cells. Further study proves that it is the aberrant ROS levels as well as NRF2/SLC7A11/GSH axis dysfunction accounting for the specific anti-tumor effects of APR-246. Mechanistically, NRF2 is specifically ubiquitylated degraded in APR-246 treated H460-Cis cells, which in turn decrease NRF2/SLC7A11/GSH axis activity.

Conclusion

Our study uncovered new insights into the biology driving cisplatin resistance of lung cancer and highlights potentials of APR-246 as future therapeutic agents again cisplatin resistance.

Background

Cancer has become a global problem and public health issue in recent decades (1, 2). As the most common malignant tumors in the world, lung cancer contributes to 1/4 of males and 1/5 of females in cancer-related deaths (1-5). In China, both the incidence and mortality of lung cancer rank first for many years (3, 6, 7). Epidemiological data reveals that serious air pollution, high rate of smoking, the increase of aging, as well as difficulties to diagnose in the early stage and insufficient cure in the late stage account for this phenomenon (6, 7). Currently, surgery, chemotherapy, TKI-based targeted therapy and

immunotherapy are main therapies of lung cancer (8-10). Despite of high rate of resistance, cisplatin-base chemotherapy is still the main treatment in lung cancer patients who are not suitable for surgery, TKI-based targeted therapy and immunotherapy (9, 11).

As the most commonly used platinum-based chemotherapeutic drug, cisplatin exhibits effective and broad-spectrum anti-tumor activity against multiple cancers, including bladder cancer, ovarian cancer, breast cancer, testicular cancer as well as lung cancer (12, 13). As a platinum-based drug, cisplatin can cross-link with DNA and subsequently inhibit DNA replication and transcription then trigger the apoptosis pathway (14, 15). Despite its widely usage, cisplatin resistance has become a major obstacle for the clinical use of cisplatin in cancer patients. Several mechanisms that account for the cisplatin-resistant phenotype of tumor cells have been described: (i) pre-target resistance, (ii) on-target resistance, (iii) post-target resistance and (iv) off-target resistance (15, 16). Therefore, attenuation of the acquired chemoresistance to cisplatin is an important and urgently needed clinical objective.

Aberrant reactive oxygen species (ROS) are found in cisplatin resistant cell lines by several research groups, indicating essential roles of ROS in cisplatin resistance (17-20). Here, we detect ROS levels in both cisplatin resistance and control H460 cells, then assess the anti-tumor activity of APR-246 based on series *in vitro* and *in vivo* experiments. Results indicates NADPH metabolism and ROS levels are the main causes accounting for cisplatin resistance of H460. Besides, APR-246 can selectively inhibit proliferation and colony formation of H460-Cis instead of H460 through mitochondria mediated apoptosis. Mechanistically, NRF2 is specifically ubiquitylated degraded in APR-246 treated H460-Cis cells, which in turn decrease NRF2/SLC7A11/GSH axis activity. In short, our study uncovered new insights into the biology driving cisplatin resistance of lung cancer and highlighted potentials of APR-246 as a future therapeutic agent again cisplatin resistance.

Materials And Methods

Cell culture

NCI-H460 (RRID:CVCL_0459, H460 for short) and H460-Cis cells were purchased from the Shanghai Cell Collection (Chinese Academy of Sciences). Both cell lines were maintained in Dulbecco's modified Eagle's medium (Gibco, Grand Island, NY, USA). All media were supplemented with 10% fetal bovine serum (Hyclone, Logan, UT, USA). H460-Cis cells are treated with 2 mg/ml cisplatin to maintain cisplatin resistance character. All human cell lines have been authenticated using STR profiling within the last three years has been included. Cells were maintained at 37°C in a humidified atmosphere with 5% CO_2. Cells were regularly tested for mycoplasma and were mycoplasma free as previously reported (21).

Reagents

APR-246 and MG132 were purchased from MedChemExpress (China). Cycloheximide (CHX) was purchase from MP Biomedicals (France). N-acetyl-L-cysteine (NAC) was bought from Beyotime

Biotechnology (Beijing, China). Each reagent was dissolved in its favorable solvent liquid at appropriated concentration. All the reagents were stored at -20°C for long-term preservation.

Quantification of ROS level

ROS was assayed using 2',7'-dichlorofluorescin diacetate (DCFDA) cellular ROS detection assay kit (Beyotime Biotechnology, Beijing, China) following manufacturers' protocol. In short, cells were seeded in 6-well plates. Then DCFDA was added to the medium 1:500 and incubated for 30 min then cells were harvested and analyzed using flow cytometry (BD Biosciences, Mississauga, Ontario). All experiments were performed in triple times.

Quantification of $NADP^+$/NADPH

The intracellular $NADP^+$ and NADPH levels were measured using the $NADP^+$/NADPH Assay Kit (Abcam, Inc., MA, USA). Experiments were performed according to the manufacturer's protocols, and the $NADP^+$, and NADPH concentrations were determined colorimetrically based on absorbance at 565 nm. All experiments were performed in triple times.

Quantification of GSH and GSSG

Total (GS), oxidized (GSSG) and reduced (GSH) glutathione concentrations were measured using the GSH/GSSG Ratio Detection Assay Kit (Abcam, Inc., MA, USA) and a fluorescence microplate reader with excitation and emission wavelengths of 490 and 520 nm, respectively. All experiments were performed in triple times.

MTT assay

Same as before (22), cells at a concentration of 5×10^4 cells/well were seeded in 100 µl culture medium into microplates (tissue culture grade, 96 wells), and the microplates were incubated in cell cultures for 72 hours or 96 hours at 37°C and 5% CO2. After the incubation period, 10 µl of the MTT labeling reagents (final concentration 0.5 mg/ml) were added to each well at preset time points, including 0 hour, 24 hours, 48 hours and 72 hours. Then we incubated the microplate for 4 h in a humidified atmosphere. And 4 hours later, 100 µl of the solubilization solution was added into each well. After hatching in the incubator overnight, we checked for complete solubilization of the purple formazan crystals and measure the absorbance of the samples using a microplate reader. The wavelength to measure absorbance of the formazan product is between 570 nm.

Colony formation assays

Briefly, cells were trypsinized, suspended in complete medium, then counted and re-plated in six-well plate to allow formation of macroscopic colonies. Plates were incubated at 37°C for 7 to 20 days, fixed with methanol, stained with crystal violet, and colonies containing at least 50 cells in size were counted.

Apoptosis and cell cycle assay

In apoptosis assay, cells were classified into different groups, according to combination of APR-246 and/or NAC. Then nonadherent and adherent cells were collected at 48 hr after treatment. Apoptosis was determined using the Alexa Fluor 488 annexin V/Dead Cell Apoptosis Kit (Roche, USA) with FACS Calibur flow cytometer (FCM) (BD Biosciences, Mississauga, Ontario). For cell cycle analyses, cells were dyed with PI and detected with the FACS Calibur FCM.

Reverse-transcription PCR and real-time PCR assay

RNA extraction and RT-PCR were performed as described previously (23). Total RNA was extracted with TRIZOL reagents following the manufacturer's instructions (Invitrogen, Carlsbad, CA, USA). Potential DNA contamination was removed by RNase-free DNase treatment (Promega, Madison, WI, USA). cDNA was prepared with the MMLV Reverse Transcriptase (Takara, Japan). Relative quantitation was determined using the ABI QuantStudio6Flex System (Thermo Fisher, USA). Primer sequences were provided in Supplemental Table 1. All the experiments were performed in triplicate.

Western blotting

Western blotting analysis were performed as described previously (24). Equal amounts of protein extracts were separated by SDS-polyacrylamide gel, transferred to a polyvinyl difluoride membrane (PVDF) membrane (Roche; Roche Diagnostics, Basel, Switzerland) at 37°C for 1 hour, followed by incubation with specific primary antibodies overnight at 4°C. Membranes were incubated with HRP-conjugated secondary antibodies at room temperature for 1 hour and detected using the ECL kit (Thermo Scientific, Rockford, IL, USA). The detailed sources and other information of antibodies were listed in the supplemental materials (Supplemental Table 2).

CHX-mediated chase assay

To assess protein stability, cells were treated with 200 μg/mL CHX to stop de novo protein synthesis. At the preset time points, cell lysates were harvested and then subjected to immunoblotting.

Primers and antibody

The detailed information of primers and antibodies were documented in the supplementary information (Supplemental Table1 and Supplemental Table 2).

Xenograft

Female BALB/c nude mice (4~5 weeks of age) were housed in the Shandong Cancer Hospital and Institute according to protocols approved by the Shandong Cancer Hospital Animal Care Committee. For xenografts, about 6.0×10^6 viable cells in 100 μl PBS were injected subcutaneously into the nude mice. Five animals per group were used in each experiment. APR-246 (50mg/kg or 100mg/kg) were injected *i.p.*

at preset timepoint. NAC (5 mg/mL) was given in the drinking water for the length of the experiment until sacrifice. Tumor sizes were measured every 4 days, and mice were euthanized when tumors reached 1.5 cm in diameter. The volume was calculated according to the formula: 1/2 × length × squared width. All studies were approved by the Animal Care Committee of Shandong Cancer Hospital.

Statistical analysis

Data from the two groups were evaluated statistically by a two-tailed unpaired t-test (GraphPad Software, San Diego, CA, USA). In these analyses, p values less than 0.05 were considered significant (*p < 0.05, **p < 0.01, ***p < 0.001).

Results

Decreased NADPH oxidase-mediated ROS accounts for cisplatin resistance of NSCLC

Cisplatin resistance is a common outcome of NSCLC patients treated with cisplatin (9, 11). Several mechanisms explaining cisplatin resistance are raised by different research groups (15, 16). In this study, we first analyzed different expressed genes from cisplatin resistant H460 cells and control cells based on high-throughput sequencing results published elsewhere (GSE21656) (25). Different expressed genes were screened out through standard pipelines, and results were displayed through volcano plot. A total of 489 genes were upregulated and 456 genes were down-regulated in H460 cisplatin resistant cells compared to control cells (Figure 1A). Related pathways of cisplatin resistant H460 cells were then analyzed by GO analysis method based on different expressed genes. Among top ranked pathways, 5 NADPH metabolism pathways were identified, including monooxygenase activity or dehydrogenase activity of different chemicals (Figure 1B). That indicated that NADPH metabolism might play critical roles in cisplatin resistance. Indeed, [NADP+]/[NADPH] ratio was significantly decreased in cisplatin resistant H460 cells (H460-Cis) (Figure 1C). As we all know, NADPH serves as the ultimate donor of reductive power for the large majority of ROS-detoxifying enzymes. Consistent with results of NADP+/NADPH quantification, ROS levels of H460-Cis was much lower than H460 cells (Figure 1D). We hypothesized that decreased NADPH oxidase-mediated ROS might accounted for cisplatin resistance of NSCLC (Figure 1E).

Effects of common chemical drugs upon both cisplatin resistant H460 cells

In order to find out novel solutions overcoming cisplatin resistance of H460-Cis cells, we screened commonly used chemical drugs and compounds by measuring survival fractions of both H460-Cis and H460 cells. Identification of chemicals specifically killing H460-Cis cells was the main aim of the screen. Carboplatin, doxorubicin, paclitaxel, 5-Fu, as well as APR-245, a commonly used p53 allosteric compounds, were enrolled in this screen. Consistent with our notion, cisplatin resistant H460 cells were also resistant to common chemical drugs including carboplatin, doxorubicin, paclitaxel (Figure 2A-2C). There was no difference between the IC50s of 5-Fu in both H460 and H460-Cis cells (Figure 2D). Only APR-246 specially killed H460-Cis cells (Figure 2E). Despite low killing efficiencies of APR-246 at low

concentration, the differences of survival fractions between H460 and H460-Cis cells were more obvious (Figure 2F). Besides, the killing effects of APR-246 in H460-Cis cells were in dose-dependent and time-dependent manners (Figure 2G-2H).

APR-246 specifically inhibited proliferation of H460-Cis cells through disrupting cell cycle

As shown in Figure 3B, APR-246 specially inhibited proliferation of H460-Cis cells at 50 μM and 100 μM. However, there was no differences in H460 cells among different groups (Figure 3A). Colony formation assay was also performed. Consistent with previous results, APR-246 could kill both H460 and H460-Cis cells. However, APR-246 displayed more significant inhibiting effects in H460-Cis cells than H460 cells (Figure 3C-3D). Results of cell cycle indicated that APR-246 specially arrested H460-Cis cells at G0/G1 phase (Figure 3E-3F). Also, percentage of S phase H460-Cis cells was much lower compared to untreated groups based on cell cycle results (Figure 3F). EdU incorporation assay was also performed. As shown in Figure 3H, EdU incorporation rate of APR-246 treated group was much lower than untreated groups in H460-Cis cells. Although changes of EdU incorporation rate were also detected between APR-246 treated and untreated H460 cells, the effects were less than that H460-Cis cells (Figure 3G-3H).

APR-246 leaded to mitochondria mediated apoptosis in cisplatin resistance cells

Apoptosis mediated by mitochondria dysfunction was a main outcome of cancer cells under treatment of chemical drugs (26-28). A distinctive feature of the early stages of programmed cell death is the disruption of active mitochondria. In this part, JC-1 assay was performed to detect early changes in mitochondria by flow cytometry. As shown in Figure 4A-4B, APR-246 only leaded to severe mitochondria dysfunctions in H460-Cis cells in dose-dependent manners. Different APR-246 treating groups of H460 cells showed no difference (Figure 4A). Apoptosis were also examined. Consistent with changes of mitochondria, APR-246 increased apoptosis, especially early-stage apoptosis, only in H460-Cis cells instead of H460 cells (Figure 4C-4D). Protein levels of cleaved PARP, cleaved Caspase-3, cleaved Caspase-7 and cleaved Caspase-9 were significantly increased after treatment of APR-246 in H460-Cis cells (Figure 4E-4F). All these results confirmed that APR-246 could lead to mitochondria mediated apoptosis in H460-Cis cells.

APR-246 disrupted NRF2/SLC7A11/GSH axis through mediating NRF-2 degradation

In the first part of this study, we showed that ROS levels of H460-Cis was much lower than H460 cells (Figure 1D). However, the changes of ROS after APR-246 treatment were unclear. So, we examined ROS changes in both APR-246 treating H460 and H460-Cis cells. Consistent with previous results, there were no changes among APR-246 treating and control groups of H460 cells (Figure 5A). However, APR-246 did aggravate ROS levels significantly in H460-Cis cells, especially at higher concentration (Figure 5B). Considering important roles of APR-246 in mediating GSH metabolism, GSH/GSSG ratios were also examined. Consistent with previous findings, APR-246 leaded severe decrease of GSH/GSSG ratios only in H460-Cis cells (Figure 5C). In order to verify molecular mechanisms of this phenomenon, SLC7A11, the main target of APR-246, was detected at both mRNA and protein levels (Figure 5D). As shown in Figure

5D, the amount of SLC7A11 in H460-Cis cells was much lower than that of H460 cells at both transcript and protein levels, indicting *SLC7A11*'s transcription might be disrupted by APR-246 treatment. The transcription factor nuclear factor erythroid 2-related factor 2 (NRF2) is the master regulator of neutralizing cellular ROS and restoring redox balance (29). Indeed, there was obvious NRF2' binding peaks at the promoter of *SLC7A11* based on experiments collected by ENCODE database (Figure 5E). It indicated that NRF2 might be the core transcription factor of SLC7A11. Consistent with expression differences of SLC7A11 between H460-Cis and H460 cells, H460-Cis cells possessed a small amount of NRF2 compared to H460 cells (Figure 5F). Moreover, NRF2 was downregulated after APR-246 treatment in H460-Cis cells (Figure 5G). To exclude detailed mechanism of NRF2 downregulation, we detected mRNA levels of *NFE2L2* (NRF2 coding gene) after APR-246 treatment at different time-point. No changes of NRF2 mRNA were detected (Figure S1). However, the downregulation of NRF2 after APR-246 treatment of H460-Cis could be totally rescued by MG132 (Figure 5H). It revealed that 26S proteasome mediated degradation of NRF2 accounted to its decrease after APR-246 treatment in H460-Cis cells. To further exclude whether APR-246 regulates NRF2 degradation, we examined NRF2 expression in H460-Cis cells treated with the protein synthesis inhibitor CHX as well as APR-246 or not. It was found that the NRF2 protein levels decreased much faster in H460-Cis cells treated with APR-246 than those treated with DMSO (Figure 5I). All these results indicated that APR-246 could disrupted ROS-related NRF2/SLC7A11/GSH axis through mediating NRF-2 degradation.

ROS accounted for anti-tumor activity of APR-246 in cisplatin resistance cells

To further confirm whether APR-246 specially inhibits H460-Cis cells through mediating ROS levels, we performed serial rescue experiments. N-Acetylcysteine (NAC), a common ROS scavenger, was used in this part. As shown in Figure 6A, NAC could disrupt inhibited proliferation of H460-Cis cells caused by APR-246. Further analysis of apoptosis also confirmed this notion. Despite APR-246 leads severe early-stage apoptosis, NAC could significantly reduce apoptosis rates to normal levels in APR-246 treating H460-Cis cells (Figure 6B). Besides, our colony formation results also demonstrated that NAC could totally eliminate inhibiting effects of APR-246 in H460-Cis cells (Figure 6C). We next evaluated the *in vivo* role of APR-246 using H460-Cis xenografts. Consistent with *in vitro* results, growth of xenografts treated with APR-246 (both low and high concentration) were severely impaired compared to the control group ($P < 0.001$), while tumors of xenografts treating with both APR-246 (high concentration) and NAC were much similar to these of controls (Figure 6D-6G).

Discussion

Inherent and acquired cisplatin resistance reduces the effectiveness of this agent in the management of non-small cell lung cancer (NSCLC) (9, 11, 30). Thus, understanding the molecular mechanisms underlying this process may result in the development of novel agents to enhance the sensitivity of cisplatin. In this study, we screened compounds overcoming cisplatin resistance based on a small panel. APR-246 was chosen due to its lower IC50 and higher inhibiting efficiency in H460-Cis cells. Further study demonstrated that cell cycle and apoptosis were dysregulated upon APR-246 treatment in H460-Cis cells.

Mechanistically, NRF2 is specifically ubiquitylated degraded in APR-246 treated H460-Cis cells, which in turn decrease NRF2/SLC7A11/GSH axis activity. What's more, this axis could be totally impaired by ROS scavenger (NAC) (Figure 6H).

APR-246, also known as PRIMA-1^{MET}, is a small organic molecule that has been shown to restore tumor-suppressor function primarily to mutant p53 and also to induce cell death in various cancer types (31-33). APR-246 exerts its anti-tumor activity through apoptosis and autophagy (33, 34). Besides, APR-246 may also exert additional effects through p53-independent mechanisms (34-36). Among p53 independent pathways, mechanisms by which APR-246 can induce ROS accumulation by depletion of GSH, are mainly accepted (37, 38). Our results reveal that regulation of p53-independent pathway is the main function of APR-246. In details, APR-246 could disrupted ROS-related NRF2/SLC7A11/GSH axis through mediating NRF-2 degradation in H460-Cis cells.

NRF2 is an essential transcription factor that regulates an array of detoxifying and antioxidant defense gene expression (29, 39). It is activated in response to oxidative stress and induces the expression of its target genes by binding to the antioxidant response element (ARE) (40). We and other groups prove that SLC7A11 is regulated by NRF2 directly (41-43). Due to NRF2's important function, regulation of NRF2 is tightly regulated by different mechanisms. Among these, Keap1-NRF2 pathway is the major pathway regulating activity of NRF2, especially after exposure of cytoprotective responses to oxidative and electrophilic stress (44). As a core repressor protein of NRF2, Keap1 promotes its degradation by the ubiquitin proteasome pathway through direct binding to NRF2 (45-47). In our study, NRF2 is also specially degraded through ubiquitin proteasome pathway after APR-246 treatment in H460-Cis cells. However, the mechanisms for degradation of NRF2 after APR-246 treatment need further investigation. Understanding the function of this regulatory pathways may lead to effective pharmacological treatment for cisplatin resistant NSCLC patients.

Also, NADPH metabolism draws our attention all through the entire study. As we all know, NADPH serves as a source of reducing equivalents for the glutathione system, consisting of the glutathione system and the thioredoxin system. Main functions of NADPH are served by a variety of dehydrogenases (48, 49). We prove that decreased NADPH oxidase-mediated ROS may account for cisplatin resistance of NSCLC based on a published dataset (50). Besides to maintenance of NADPH, the glutathione metabolism system is also dysregulated after APR-246 treatment. This indicates important roles of NADPH and GSH metabolism in cisplatin resistance. More detailed revelation mechanisms underlying relationships between metabolism and cisplatin resistance should be considered in our further study.

In summary, we identify APR-246 as an effective anti-tumor compound especillay in cispaltin resistant NSCLC based on our screening panel. APR-246 selectively inhibits proliferation and colony formation of H460-Cis instead of H460 through mitochondria mediated apoptosis as well as cell cycle dysregulation. Mechanistically, APR-246 could disrupt ROS-related NRF2/SLC7A11/GSH axis through mediating NRF-2 degradation in H460-Cis cells. Our study uncovered new insights into the biology driving cisplatin

resistance of lung cancer and highlights potentials of APR-246 as future therapeutic agents again cisplatin resistance.

Conclusion

In summary, our data show that APR-246 is an effective anti-tumor compound especillay in cispaltin resistant NSCLC. APR-246 can obviously lead to severe mitochondria dysfunction as well as elevated apoptosis in H460-Cis cells. Further study proves that it is the aberrant ROS levels as well as NRF2/SLC7A11/GSH axis dysfunction accounting for the specific anti-tumor effects of APR-246. Mechanistically, NRF2 is specifically ubiquitylated degraded in APR-246 treated H460-Cis cells, which in turn decrease NRF2/SLC7A11/GSH axis activity. Our study uncovered new insights into the biology driving cisplatin resistance of lung cancer and highlights potentials of APR-246 as future therapeutic agents again cisplatin resistance.

List Of Abbreviations

ROS: reactive oxygen species; NADPH: nicotinamide adenine dinucleotide phosphate; TKI: tyrosine kinase inhibitor; GSH: glutathione; GSSG: oxidized glutathione; NRF2: Nuclear factor (erythroid-derived 2)-like 2; SLC7A11: Solute Carrier Family 7 (Anionic Amino Acid Transporter Light Chain, Xc- System), Member 11.

Declarations

Ethics approval and consent to participate

The study was approved by the Ethics Committee of Shandong Cancer Hospital and Institute. Animal studies in nude mice were approved by the Shandong Cancer Hospital Animal Care Committee and the Animal Care Committee of Shandong Cancer Hospital.

Consent for publication

All authors have seen and approved the manuscript and consent publication.

Availability of data and material

The datasets used and/or analyzed during the current study are available from the corresponding author on reasonable request.

Competing interests

No financial and non-financial competing interests exist in this study.

Funding

This work was supported by the National Natural Science Foundation of China (Grant No. 81702276 and 81801613), National Natural Science Foundation of Shandong Province (Grant No. ZR2016HQ48 and ZR2019LZL011), Science and Technology Development Plan of Jinan (Grant No. 201805067), Medicine and Health Care Science and Technology Development Plan Projects Foundation of Shandong Province (Grant No. 2015WSA18054 and 2019WS202), Project of Shandong Academy of Medical Sciences (Grant No. 2018-11 and 2018-28).

Authors' contributions

J.P.Y. designed experiments and helped write the manuscript; Q.X., Q.H.J., Y.Z. and W.H.M. performed the in vitro experiments; B.Q.T., Y.L.L. and Y.S.C. performed the in vivo experiments; Q.X. wrote the manuscript; F.W., X.W.W. and R.Z. contributed reagents, performed statics and edited the manuscript.

Acknowledgements

The authors are grateful to Xingguo Song for kindly providing the H460-Cis cells.

Authors' information

The Second Hospital, Cheeloo College of Medicine, Shandong University, Jinan, Shandong, 250033, P.R. China:

Qian Xin, Qinghong Ji, Ying Zhang, Weihong Ma

Shandong Cancer Hospital and Institute, Shandong First Medical University and Shandong Academy of Medical Sciences, Jinan, Shandong, 250117, P.R. China:

Baoqing Tian, Yanli Liu, Yunsong Chen, Fei Wang, Ran Zhang, Xingwu Wang, Jupeng Yuan

Corresponding authors

Correspondence to Jupeng Yuan.

References

1. de Martel C, Georges D, Bray F, Ferlay J, Clifford GM. Global burden of cancer attributable to infections in 2018: a worldwide incidence analysis. Lancet Glob Health. 2020;8(2):e180-e90.
2. Siegel RL, Miller KD, Jemal A. Cancer statistics, 2019. CA Cancer J Clin. 2019;69(1):7-34.
3. Yang D, Liu Y, Bai C, Wang X, Powell CA. Epidemiology of lung cancer and lung cancer screening programs in China and the United States. Cancer Lett. 2020;468:82-7.
4. Pastorino U, Silva M, Sestini S, Sabia F, Boeri M, Cantarutti A, et al. Prolonged lung cancer screening reduced 10-year mortality in the MILD trial: new confirmation of lung cancer screening efficacy. Ann Oncol. 2019;30(7):1162-9.

5. Vineis P, Wild CP. Global cancer patterns: causes and prevention. Lancet. 2014;383(9916):549-57.
6. Zeng H, Chen W, Zheng R, Zhang S, Ji JS, Zou X, et al. Changing cancer survival in China during 2003-15: a pooled analysis of 17 population-based cancer registries. Lancet Glob Health. 2018;6(5):e555-e67.
7. Chen W, Zheng R, Baade PD, Zhang S, Zeng H, Bray F, et al. Cancer statistics in China, 2015. CA Cancer J Clin. 2016;66(2):115-32.
8. Wu SG, Shih JY. Management of acquired resistance to EGFR TKI-targeted therapy in advanced non-small cell lung cancer. Mol Cancer. 2018;17(1):38.
9. Hirsch FR, Scagliotti GV, Mulshine JL, Kwon R, Curran WJ, Jr., Wu YL, et al. Lung cancer: current therapies and new targeted treatments. Lancet. 2017;389(10066):299-311.
10. Steven A, Fisher SA, Robinson BW. Immunotherapy for lung cancer. Respirology. 2016;21(5):821-33.
11. Kaplan JA, Liu R, Freedman JD, Padera R, Schwartz J, Colson YL, et al. Prevention of lung cancer recurrence using cisplatin-loaded superhydrophobic nanofiber meshes. Biomaterials. 2016;76:273-81.
12. Ho GY, Woodward N, Coward JI. Cisplatin versus carboplatin: comparative review of therapeutic management in solid malignancies. Crit Rev Oncol Hematol. 2016;102:37-46.
13. Barabas K, Milner R, Lurie D, Adin C. Cisplatin: a review of toxicities and therapeutic applications. Vet Comp Oncol. 2008;6(1):1-18.
14. Ghosh S. Cisplatin: The first metal based anticancer drug. Bioorg Chem. 2019;88:102925.
15. Siddik ZH. Cisplatin: mode of cytotoxic action and molecular basis of resistance. Oncogene. 2003;22(47):7265-79.
16. Galluzzi L, Senovilla L, Vitale I, Michels J, Martins I, Kepp O, et al. Molecular mechanisms of cisplatin resistance. Oncogene. 2012;31(15):1869-83.
17. Wang N, Song L, Xu Y, Zhang L, Wu Y, Guo J, et al. Loss of Scribble confers cisplatin resistance during NSCLC chemotherapy via Nox2/ROS and Nrf2/PD-L1 signaling. EBioMedicine. 2019;47:65-77.
18. Han Y, Kim B, Cho U, Park IS, Kim SI, Dhanasekaran DN, et al. Mitochondrial fission causes cisplatin resistance under hypoxic conditions via ROS in ovarian cancer cells. Oncogene. 2019;38(45):7089-105.
19. Meng Y, Chen CW, Yung MMH, Sun W, Sun J, Li Z, et al. DUOXA1-mediated ROS production promotes cisplatin resistance by activating ATR-Chk1 pathway in ovarian cancer. Cancer Lett. 2018;428:104-16.
20. Kim EH, Jang H, Shin D, Baek SH, Roh JL. Targeting Nrf2 with wogonin overcomes cisplatin resistance in head and neck cancer. Apoptosis. 2016;21(11):1265-78.
21. Yuan J, Song Y, Pan W, Li Y, Xu Y, Xie M, et al. LncRNA SLC26A4-AS1 suppresses the MRN complex-mediated DNA repair signaling and thyroid cancer metastasis by destabilizing DDX5. Oncogene. 2020;39(43):6664-76.

22. Yuan J, Han B, Hu H, Qian Y, Liu Z, Wei Z, et al. CUL4B activates Wnt/beta-catenin signalling in hepatocellular carcinoma by repressing Wnt antagonists. J Pathol. 2015;235(5):784-95.
23. Qian Y, Yuan J, Hu H, Yang Q, Li J, Zhang S, et al. The CUL4B/AKT/beta-Catenin Axis Restricts the Accumulation of Myeloid-Derived Suppressor Cells to Prohibit the Establishment of a Tumor-Permissive Microenvironment. Cancer Res. 2015;75(23):5070-83.
24. Xin Q, Li J, Dang J, Bian X, Shan S, Yuan J, et al. miR-155 Deficiency Ameliorates Autoimmune Inflammation of Systemic Lupus Erythematosus by Targeting S1pr1 in Faslpr/lpr Mice. J Immunol. 2015;194(11):5437-45.
25. Sun Y, Zheng S, Torossian A, Speirs CK, Schleicher S, Giacalone NJ, et al. Role of insulin-like growth factor-1 signaling pathway in cisplatin-resistant lung cancer cells. Int J Radiat Oncol Biol Phys. 2012;82(3):e563-72.
26. Porporato PE, Filigheddu N, Pedro JMB, Kroemer G, Galluzzi L. Mitochondrial metabolism and cancer. Cell Res. 2018;28(3):265-80.
27. Dickerson T, Jauregui CE, Teng Y. Friend or foe? Mitochondria as a pharmacological target in cancer treatment. Future Med Chem. 2017;9(18):2197-210.
28. Zong WX, Rabinowitz JD, White E. Mitochondria and Cancer. Mol Cell. 2016;61(5):667-76.
29. Shelton P, Jaiswal AK. The transcription factor NF-E2-related factor 2 (Nrf2): a protooncogene? FASEB J. 2013;27(2):414-23.
30. Barr MP, Gray SG, Hoffmann AC, Hilger RA, Thomale J, O'Flaherty JD, et al. Generation and characterisation of cisplatin-resistant non-small cell lung cancer cell lines displaying a stem-like signature. PLoS One. 2013;8(1):e54193.
31. Rokaeus N, Shen J, Eckhardt I, Bykov VJ, Wiman KG, Wilhelm MT. PRIMA-1(MET)/APR-246 targets mutant forms of p53 family members p63 and p73. Oncogene. 2010;29(49):6442-51.
32. Wiman KG. Pharmacological reactivation of mutant p53: from protein structure to the cancer patient. Oncogene. 2010;29(30):4245-52.
33. Shen J, Vakifahmetoglu H, Stridh H, Zhivotovsky B, Wiman KG. PRIMA-1MET induces mitochondrial apoptosis through activation of caspase-2. Oncogene. 2008;27(51):6571-80.
34. Grellety T, Laroche-Clary A, Chaire V, Lagarde P, Chibon F, Neuville A, et al. PRIMA-1(MET) induces death in soft-tissue sarcomas cell independent of p53. BMC Cancer. 2015;15:684.
35. Liu DS, Read M, Cullinane C, Azar WJ, Fennell CM, Montgomery KG, et al. APR-246 potently inhibits tumour growth and overcomes chemoresistance in preclinical models of oesophageal adenocarcinoma. Gut. 2015;64(10):1506-16.
36. Zandi R, Selivanova G, Christensen CL, Gerds TA, Willumsen BM, Poulsen HS. PRIMA-1Met/APR-246 induces apoptosis and tumor growth delay in small cell lung cancer expressing mutant p53. Clin Cancer Res. 2011;17(9):2830-41.
37. Ogiwara H, Takahashi K, Sasaki M, Kuroda T, Yoshida H, Watanabe R, et al. Targeting the Vulnerability of Glutathione Metabolism in ARID1A-Deficient Cancers. Cancer Cell. 2019;35(2):177-90

e8.
38. Bykov VJ, Zhang Q, Zhang M, Ceder S, Abrahmsen L, Wiman KG. Targeting of Mutant p53 and the Cellular Redox Balance by APR-246 as a Strategy for Efficient Cancer Therapy. Front Oncol. 2016;6:21.
39. Shin SM, Yang JH, Ki SH. Role of the Nrf2-ARE pathway in liver diseases. Oxid Med Cell Longev. 2013;2013:763257.
40. Yang L, Yang F, Teng L, Katayama I. 6-Shogaol Protects Human Melanocytes against Oxidative Stress through Activation of the Nrf2-Antioxidant Response Element Signaling Pathway. Int J Mol Sci. 2020;21(10).
41. Qiang Z, Dong H, Xia Y, Chai D, Hu R, Jiang H. Nrf2 and STAT3 Alleviates Ferroptosis-Mediated IIR-ALI by Regulating SLC7A11. Oxid Med Cell Longev. 2020;2020:5146982.
42. Dong H, Qiang Z, Chai D, Peng J, Xia Y, Hu R, et al. Nrf2 inhibits ferroptosis and protects against acute lung injury due to intestinal ischemia reperfusion via regulating SLC7A11 and HO-1. Aging (Albany NY). 2020;12(13):12943-59.
43. Chen D, Tavana O, Chu B, Erber L, Chen Y, Baer R, et al. NRF2 Is a Major Target of ARF in p53-Independent Tumor Suppression. Mol Cell. 2017;68(1):224-32 e4.
44. Fan Z, Wirth AK, Chen D, Wruck CJ, Rauh M, Buchfelder M, et al. Nrf2-Keap1 pathway promotes cell proliferation and diminishes ferroptosis. Oncogenesis. 2017;6(8):e371.
45. Yamamoto M, Kensler TW, Motohashi H. The KEAP1-NRF2 System: a Thiol-Based Sensor-Effector Apparatus for Maintaining Redox Homeostasis. Physiol Rev. 2018;98(3):1169-203.
46. Bellezza I, Giambanco I, Minelli A, Donato R. Nrf2-Keap1 signaling in oxidative and reductive stress. Biochim Biophys Acta Mol Cell Res. 2018;1865(5):721-33.
47. Kansanen E, Kuosmanen SM, Leinonen H, Levonen AL. The Keap1-Nrf2 pathway: Mechanisms of activation and dysregulation in cancer. Redox Biol. 2013;1:45-9.
48. Zhu Y, Dean AE, Horikoshi N, Heer C, Spitz DR, Gius D. Emerging evidence for targeting mitochondrial metabolic dysfunction in cancer therapy. J Clin Invest. 2018;128(9):3682-91.
49. Jin L, Li D, Alesi GN, Fan J, Kang HB, Lu Z, et al. Glutamate dehydrogenase 1 signals through antioxidant glutathione peroxidase 1 to regulate redox homeostasis and tumor growth. Cancer Cell. 2015;27(2):257-70.
50. Zhao M, Wang T, Hui Z. Aspirin overcomes cisplatin resistance in lung cancer by inhibiting cancer cell stemness. Thorac Cancer. 2020.

Figures

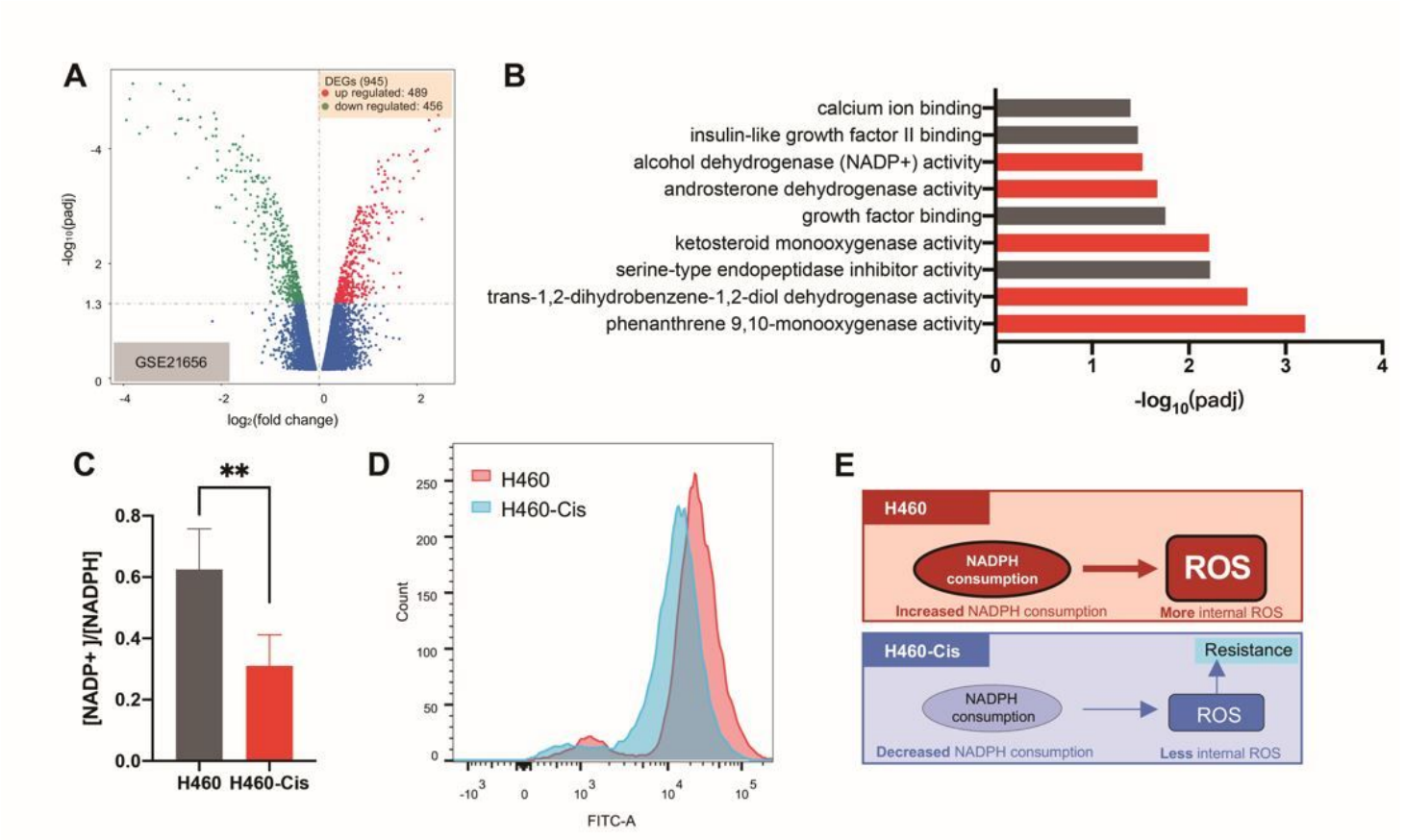

Figure 1

Role of NADPH oxidase-Mediated ROS in cisplatin resistance of NSCLC (A) Different expressed genes in cisplatin resistant H460 cells and its parental cells (GSE21656). Padj less than 0.05 are set as cut-off values. Red dots stand for upregulated genes, while downregulated genes are shown in blue dots. (B) Related pathways related to cisplatin resistance are analyzed by GO methods. Pathways belonged to NADPH metabolism are highlighted in red. (C) Quantification of NADP+ and NADPH in H460 and H460-Cis cells. (D) ROS levels of both H460 and H460-Cis cells are detected by FCS. (E) Model presenting important role of NADPH oxidase-Mediated ROS in cisplatin resistance of NSCLC. Error bars represent SD of three independent experiments. *p < 0.05; **p < 0.01; ***p < 0.001 (two-tailed unpaired t-test).

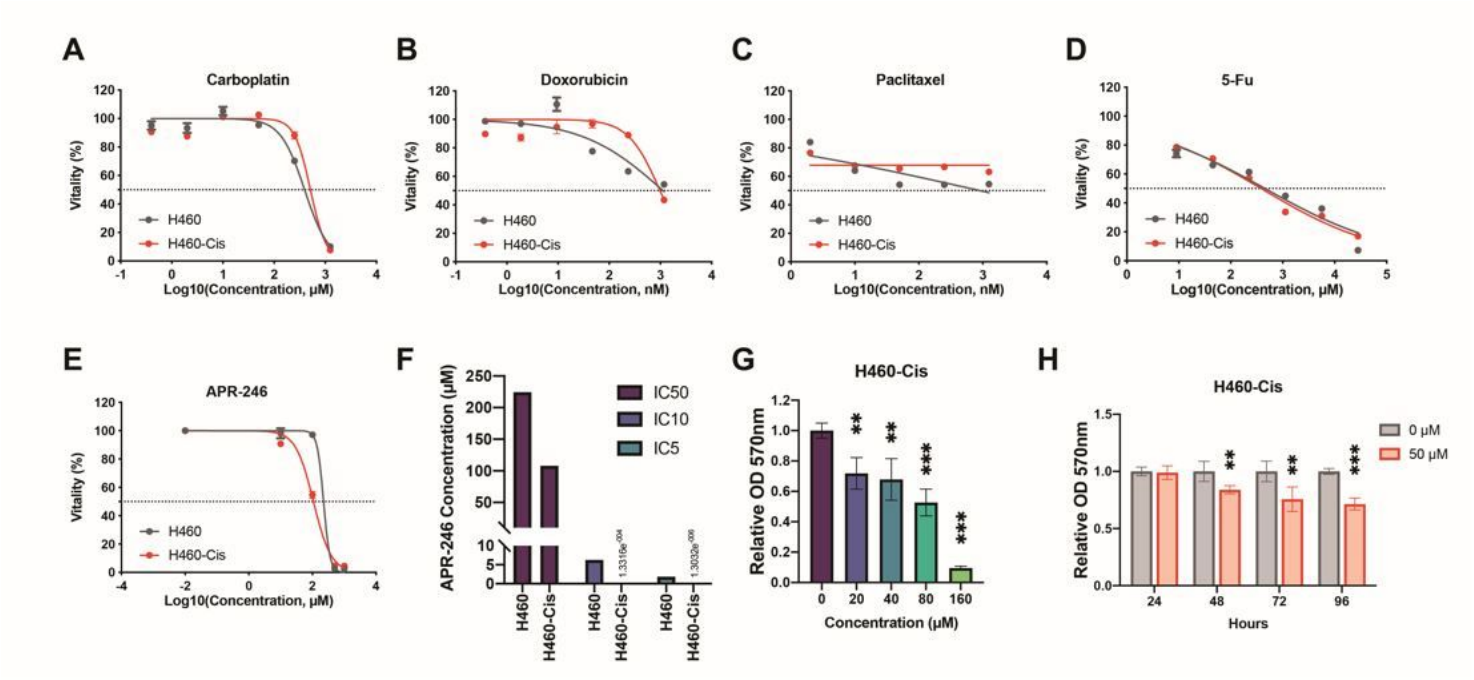

Figure 2

Anti-tumor effects of APR-246 in both H460 and H460-Cis cells (A-E) Dose response curves of carboplatin (A), doxorubicin (B), paclitaxel (C), 5-Fu (D) as well as APR-246 (E) in both H460 and H460-Cis cells. (F) IC5, IC10 and IC50 values of APR-246 in both H460 and H460-Cis cells. (G) Dose dependent anti-tumor efficiency of APR-246 in H460-Cis cells. (H) Time dependent anti-tumor efficiency of APR-246 in H460-Cis cells. Error bars represent SD of three independent experiments. *p < 0.05; **p < 0.01; ***p < 0.001 (two-tailed unpaired t-test).

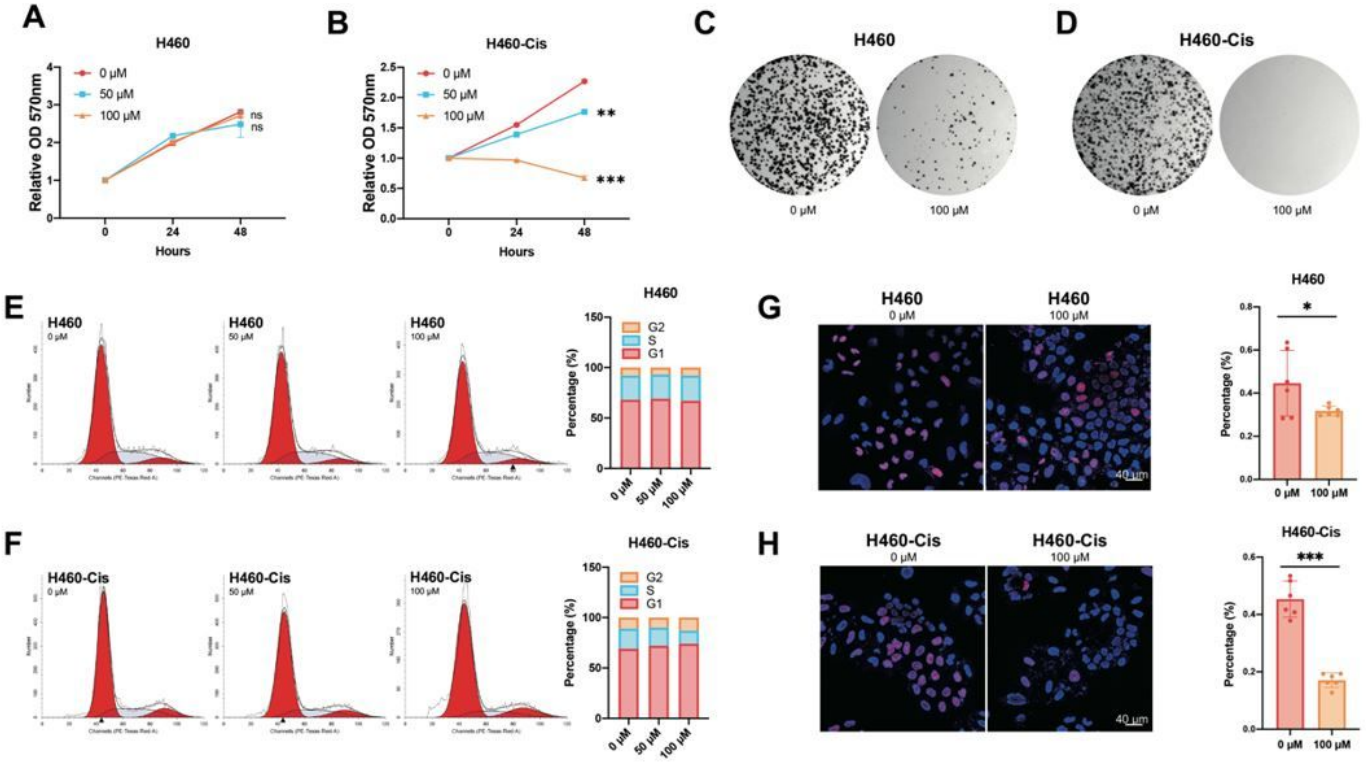

Figure 3

Dysregulation of cell cycle caused by APR-246 in H460-Cis cells (A-B) Growth cures of H460 and H460-Cis cells treated with APR-246 or not. (C-D) Colony formation assays of H460 and H460-Cis cells treated with APR-246 or not. (E-F) Cell cycle distribution of H460 and H460-Cis cells treated with APR-246 or not. (G-H) Results of EdU incorporation assay detected in APR-246 treating H460 and H460-Cis cells. Error bars represent SD of three independent experiments. *p < 0.05; **p < 0.01; ***p < 0.001 (two-tailed unpaired t-test).

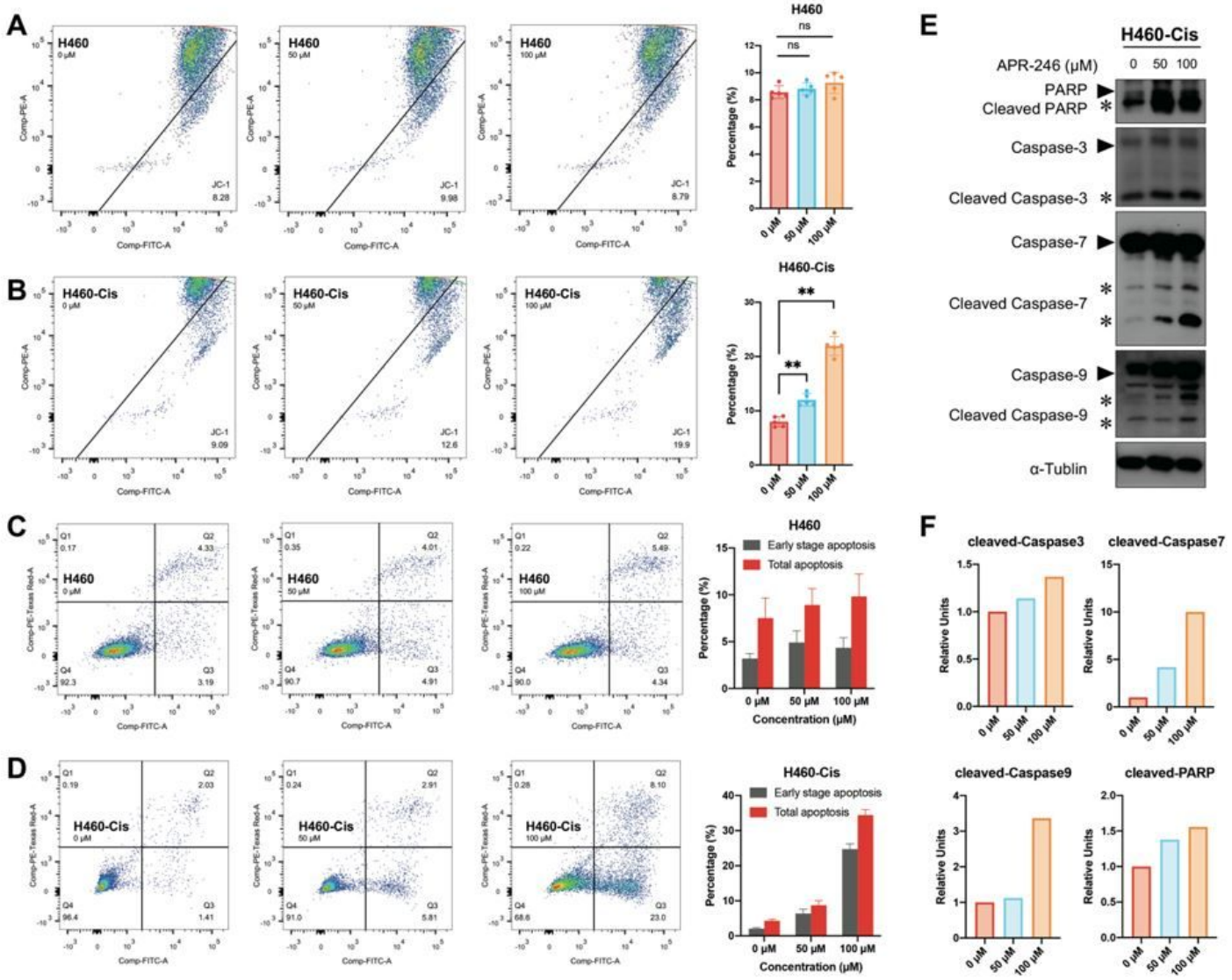

Figure 4

APR-246 leads to mitochondria mediated apoptosis in H460-Cis cells (A-B) Mitochondrial membrane potentials of H460 and H460-Cis cells treated with APR-246 are detected by JC-1 assay. Representative results are shown on the left and statistical analysis is on the right. Error bars represent the SD of three independent experiments. (C-D) Apoptosis results of H460 and H460-Cis cells treated with APR-246 or not. Representative results are shown on the left and statistical analysis is on the right. Error bars represent the SD of three independent experiments. (E) Western blotting results of PARP, Caspase-3,

Caspase-7, Caspase-9 as well as their cleaved forms. (F) Protein levels of cleaved PARP, cleaved Caspase-3, cleaved Caspase-7, cleaved Caspase-9 are quantified by densitometric analysis using Quantity One. Error bars represent SD of three independent experiments. *p < 0.05; **p < 0.01; ***p < 0.001 (two-tailed unpaired t-test).

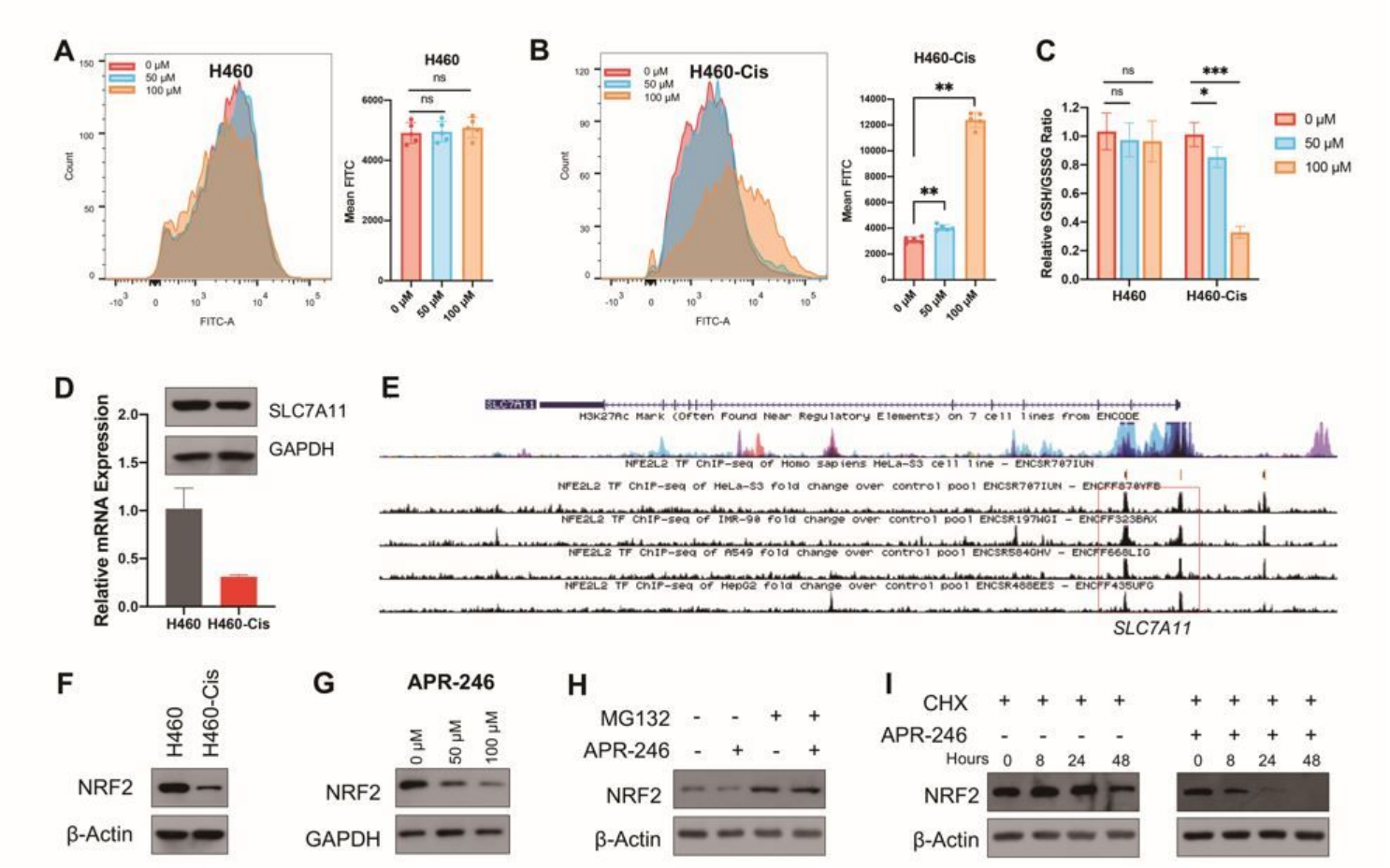

Figure 5

APR-246 promotes NRF2 degradation and alerts NRF2/SLC7A11/GSH axis (A-B) Detection of ROS levels in APR-246 treating H460 and H460-Cis cells by FCS. Representative results are shown on the left and statistical analysis is on the right. Error bars represent the SD of three independent experiments. (C) GSH and GSSG levels detected in both H460 and H460-Cis cells treated with APR-246 or not. (D) Protein and mRNA levels of SLC7A11 in H460 and H460-Cis cells. The upper panel stands for Western blotting results, while real-time PCR results are shown in the lower panel. (E) ChIP-sequencing results of NRF2 and H3K27Ac are shown by UCSC browser. Binding peaks of NRF2 at SLC7A11's promoter is highlighted within the red box. (F) Protein levels of NRF2 in H460 and H460-Cis cells are detected by Western blotting. (G) Western blotting results of NRF2 in both APR-246 treating H460-Cis and control cells. (H) Western blotting of whole cell lysates of the indicated cells treated with or without 30 μM MG132 for 24 h. (I) APR-246 treating H460-Cis and control cells are treated with 50 μg/ml cycloheximide, harvested at the indicated time points, and then subjected to Western blotting. Error bars represent SD of three independent experiments. *p < 0.05; **p < 0.01; ***p < 0.001 (two-tailed unpaired t-test).

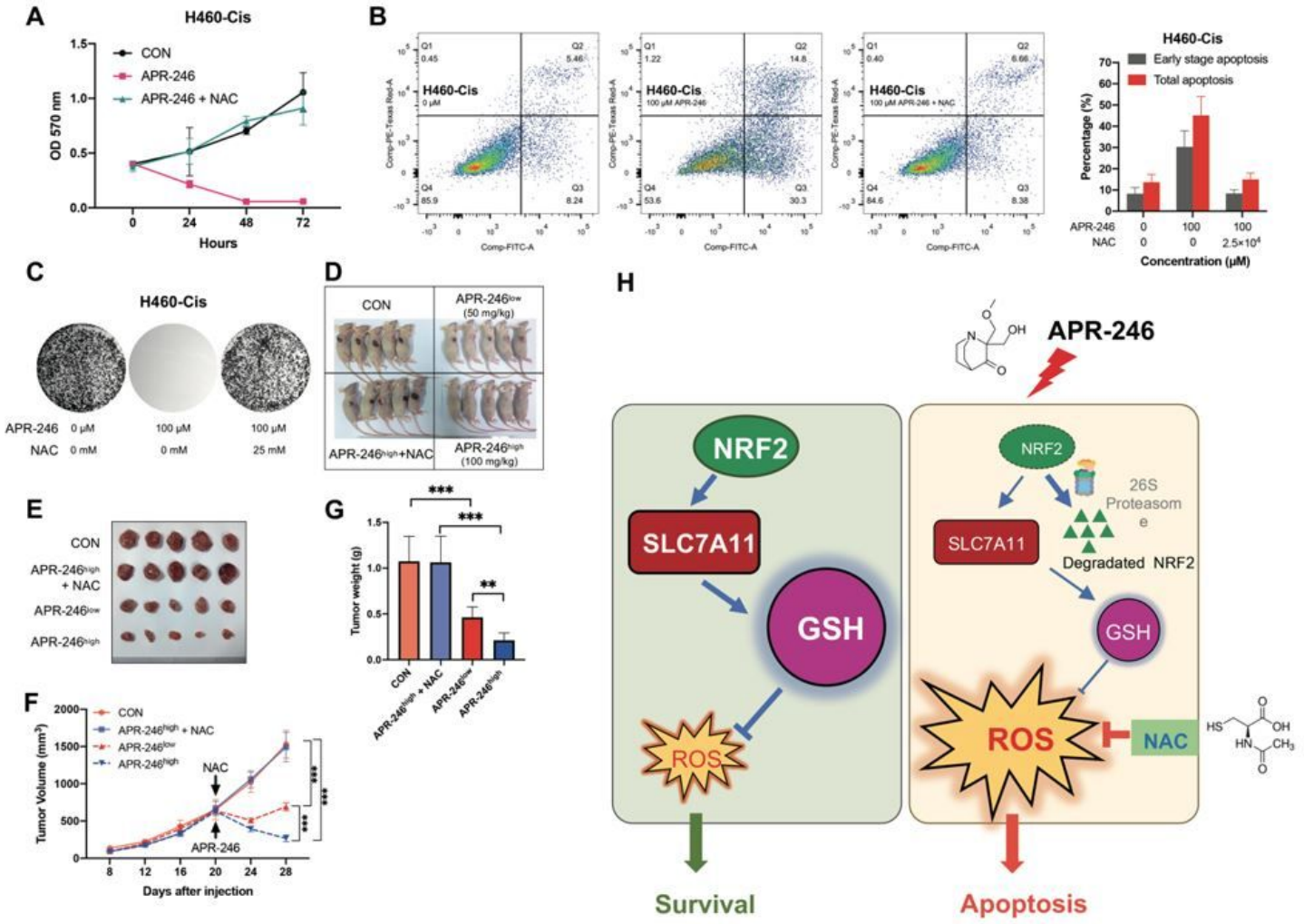

Figure 6

NAC disrupts anti-tumor effects of APR-246 (A) Proliferation of H460-Cis cells treated with APR-246 or/and NAC. (B) Apoptosis levels of H460-Cis cells treated with APR-246 or/and NAC are detected by FCS. The right panel stands for statistical analysis results. Error bars represent the SD of three independent experiments. (C) Colony formation efficiency of H460-Cis cells treated with APR-246 or/and NAC. (D-G) Xenograft of H460-Cis cells treated with APR-246 or/and NAC (n=5 per group). The size of tumor is measured every 4 days after transplantation starting at day 8. Photos of tumors are shown in (D-E). Tumor growth curves and tumor weights are provided in (F-G). Each group contained five mice. Error bars represent the SEM. APR-246 (50mg/kg or 100mg/kg) were injected i.p. at preset timepoint. NAC (5 mg/mL) was given in the drinking water for the length of the experiment until sacrifice. (H) Graphical representation of the relationship between APR-246 and cisplatin resistance of NSCLC *p < 0.05; **p < 0.01; ***p < 0.001 (two-tailed unpaired t-test).

Supplementary Files

This is a list of supplementary files associated with this preprint. Click to download.

- AbstractGraphic.png
- SupplementalInformation.docx